Chinese Journal of Polymer Science Vol. 33, No. 2, (2015), 349–361

Chinese Journal of Polymer Science
© Chinese Chemical Society
Institute of Chemistry, CAS
Springer-Verlag Berlin Heidelberg 2015

Crystallization Kinetics and Morphology of Poly(vinylidene fluoride)/Poly(ethylene adipate) Blends*

Hai-jun Wang[a**], Hui-ping Feng[a, b], Xue-chuan Wang[a], Qing-chuan Du[c] and Chao Yan[c]

[a] *Shaanxi University of Science and Technology, Xi'an 710021, China*

[b] *Shaanxi Research Institute of Agricultural Products Processing Technology, Xi'an 710021, China*

[c] *School of Material Science & Engineering, Jiangsu University of Science and Technology, Zhenjiang 212003, China*

Abstract The miscibility, isothermal crystallization kinetics and morphology of the poly(vinylidene fluoride) (PVDF)/poly(ethylene adipate) (PEA) blends have been studied by differential scanning calorimetry (DSC), optical microscopy (OM) and scanning electron microscopy (SEM). A depression of the equilibrium melting point of PVDF was observed. From the melting point data of PVDF, a negative but quite small value of the interaction parameter $\chi_{PVDF\text{-}PEA}$ is derived using the Flory-Huggins equation, implying that PVDF shows miscibility with PEA to some extent. Nonisothermal and isothermal crystallization kinetics suggest that the crystallization rate of PVDF decreases with increasing the amount of PEA, and a contrary trend was found when PEA crystallizes with the increase of the amount of PVDF. It was further disclosed that the blend ratio and crystallization temperature affect the texture of PVDF spherulites greatly, which determines the subsequent crystallization of PEA. At high temperatures, *e.g.* 150 °C, the band spacing of PVDF spherulites increases with the addition of PEA content and the spherulitic structure becomes more open. In this case, spherulitic crystallization of PEA is not observed for all blend compositions. At low temperatures, *e.g.* 130 °C, for the PEA-rich blends, the interpenetrated structures are eventually formed by the penetration of the spherulites of PEA growing within the pre-existing PVDF spherulites.

Keywords: Crystallization; Thermodynamic properties; Blends; Poly(vinylidene fluoride); Poly(ethylene adipate).

INTRODUCTION

As a simple means for producing new polymeric materials with desirable properties, blending one polymeric material with another is of scientific and industrial interest. Binary polymer systems may be of crystalline/crystalline, crystalline/amorphous and amorphous/amorphous blend types[1–4]. A growing number of commercial materials are crystalline/crystalline polymer blends, which often exhibit more excellent mechanical properties and environmental resistance than the other two types. Although many crystalline/crystalline polymer blend systems have been studied, the crystallization and morphology development of binary miscible crystalline polymer blends, especially one of the components has a lower melting point (T_m), are not well understood in neat semicrystalline materials.

One semicrystalline polymer that has been widely used as a high melting point blend component is poly(vinylidene fluoride) (PVDF). PVDF has been extensively studied for its various applications to ferroelectric polymer devices[5]. PVDF is known to be a semicrystalline polymer with polymorphs, the

* This work was financially supported by the National Natural Science Foundation of China (Nos. 21204045, 21276151), Key Scientific Research Group of Shanxi Province (No. 2013KCT-08) and Scientific Research Group of Shanxi University of Science and Technology (No. TD12-04).

** Corresponding author: Hai-jun Wang (王海军), E-mail: wanghaijun@sust.edu.cn

Received June 11, 2014; Revised July 22, 2014; Accepted July 28, 2014
doi: 10.1007/s10118-015-1585-3

occurrence of which strongly depends on the processing conditions. Crystallization of PVDF from the melt yields two types of spherulites. The most common α-form consists of large, highly birefringent, and tightly banded spherulites, which are induced at large supercoolings. The γ polymorphic form, obtained in specimens crystallized at very high temperatures, exhibits irregular or disorganized birefringent and lamellar scrolling features[6]. So far, lots of polymer blends comprising of PVDF have been studied, such as PVDF/poly(methyl methacrylate) (PMMA)[7–10], PVDF/poly(vinyl acetate) (PVA-c)[11], PVDF/ethylene-vinylacetate copolymers (EVAc)[12], PVDF/poly(ethylene terephthalate) (PET)[13], PVDF/Nylon-6[14] and PVDF/poly(butylene adipate) (PBA)[15–18]. Most frequently, the crystallization kinetics and morphological developments of the PVDF component were studied using optical microscopy, scattering and diffraction, and spectroscopies.

Recently, however, more attentions have been paid to the crystallization and morphology of the other low-T_m component, which is affected not only by the crystallization temperature and blend ratios, but also strongly by the pre-existing crystal framework of PVDF[19–23]. Through optical microscopy observation, Lee *et al*. found that the crystallization behaviors of poly(butylenes succinate) (PBS) are influenced strongly by the presence of pre-existing spherulitic PVDF crystals[19]. Qiu *et al*. studied the crystallization behaviors of poly(butylenes succinate-*co*-butylene adipate) (PBSA) and poly(3-hydroxybutyrate-*co*-hydroxyvalerate) (PHBV) in the PVDF matrix and found that both of the two low-T_m components exhibit the spherulitic morphology within the matrix of the pre-existing PVDF crystals[20, 21]. Wang *et al.* studied the confined crystallization process of PBS in PVDF/PBS blends using atomic force microscopy and found that PBS crystal lamellae nucleate and grow inside the matrix of PVDF spherulites[22, 23]. The interconnection of the molten pockets within the PVDF spherulites, which depends on the PVDF crystallization temperature, determines the growth kinetics of PBS confined within the PVDF scaffold. Furthermore, it was also found that the polymorphic crystalline structure of the low-T_m component can be regulated by blending with PVDF[18].

It is well known that the crystalline structure and morphology play an important role in the physical properties of polymers. Therefore, more attention should be paid to the crystallization kinetics since it greatly affects the crystalline structure[24]. However, the crystallization kinetics and morphology of PVDF in binary crystalline polymer blends, especially in those partially miscible or immiscible blends, are far away from being well understood till now. In the present paper, PVDF and poly(ethylene adipate) (PEA) have been chosen for detailed characterization of the crystallization kinetics and morphology under various blend ratios and isothermal crystallization conditions. PEA is a type of aliphatic polyester, which has a similar structure of $(-O-(CH_2)_2-O-CO-(CH_2)_4-CO-)_n$ with that of PBS and PBA[25]. Miscibility in blends of PVDF and PBA[16], PVDF and PBS[22, 23] has been reported. However, PVDF/PEA blends were classified as immiscible[26]. The main objective of this research is to determine the miscibility and quantitatively analyze the influence of blend composition on isothermal crystallization kinetics of PVDF/PEA blends. The morphology of the blend is observed by scanning electron microscopy (SEM) and optical microscopy (OM). The crystallization behaviors of PVDF and PEA are investigated by differential scanning calorimetry (DSC). Crystallization kinetics parameters based on the isothermal crystallization are analyzed according to the Avrami equation.

EXPERIMENTAL

Materials

PVDF (M_w = 275000 g/mol, M_n = 107000 g/mol) and PEA (M_w = 10000 g/mol) were purchased from Sigma-Aldrich Company. The melting points were measured to be 174 °C for PVDF and 47 °C for PEA. Both of them were used without further purification.

Preparation

Blends of PVDF and PEA were prepared by solution blending. Both of them were dissolved in *N*,*N*-dimethyl formamide (DMF), which served as a common solvent, with desired mass proportions (total polymer concentration was 5 mg/mL). Thin films for optical microscopy (OM) and scanning electron microscopy (SEM) observations were prepared by solution casting on glass slides. The thickness of the result films was estimated to

be 5–10 μm. The obtained films for OM and SEM were heat-treated at 190 °C for 5 min to erase the thermal history of the samples and then cooled to predetermined isothermal crystallization temperature for 72 h to ensure complete crystallization. For SEM, the films were immersed for 48 h in chloroform at room temperature to etch away PEA. Etching was necessary because the lamellar bundles of PVDF were buried in PEA and almost invisible. After etching, the lamellar morphologies of PVDF emerged.

Characterizations

Thermal analysis was performed using a TA Instruments differential scanning calorimetry (DSC) Q100 with a Universal Analysis 2000. An Olympus BH-2 microscopy equipped with a Linkam LK-600 PM temperature controller was used to observe the crystalline morphology. All of the optical micrographs shown in this paper were taken under crossed polarizers. The fine morphologies of PVDF/PEA blends were examined and characterized using a Field Emission Scanning Electron Microscope (Hitachi S-4800) operated at accelerating voltage of 2.0 kV.

RESULTS AND DISCUSSION

Miscibility Study of PVDF/PEA Blends

Glass transition temperature (T_g) is the most efficient index to evaluate the miscibility of binary blends. However, the glass transition temperature (T_g) of PVDF is –43.1 °C and that of PEA is –52.7 °C. Because of the proximity of T_gs of the two components, the miscibility of PVDF/PEA blends could not be determined by measuring T_g of the blend conveniently as usual. Another important method in understanding the miscibility of a polymer blend system is to analyze the melting behavior of a crystalline component[27]. In miscible blends, the depression of the melting point of the crystalline component is an important characteristic presenting polymer compatibility caused by thermodynamically favorable interactions. Therefore, the miscibility of PVDF/PEA blends is evaluated by studying the equilibrium melting point of PVDF.

Figure 1 shows the DSC melting curves of PVDF in PVDF/PEA blends after melt-crystallized at 150 °C. It is evident from Fig. 1 that the melting endothermal peak of PVDF decreases with increasing PEA content. The depression of the melting point of PVDF in PVDF/PEA blends is in general affected not only by thermodynamic factors but also by morphological parameters such as the crystal thickness[15]. The equilibrium melting temperature is defined as the melting point of the infinity large lamella, which can eliminate morphological disturbances. For a miscible blend, a marked depression of the equilibrium melting temperature can only be

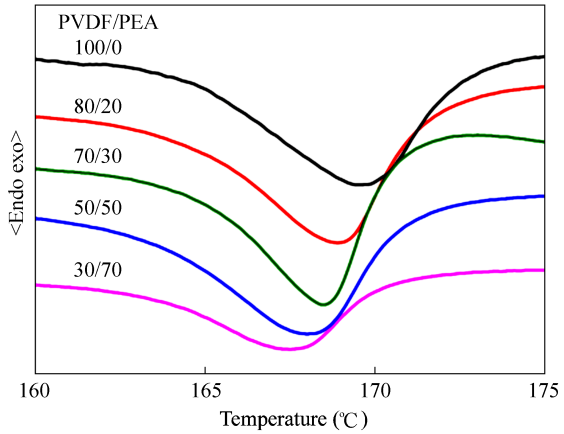


Fig. 1 DSC heating thermograms of PVDF-PEA blends isothermally crystallized at 150 °C for 48 h (Scan rate is 10 K/min.)

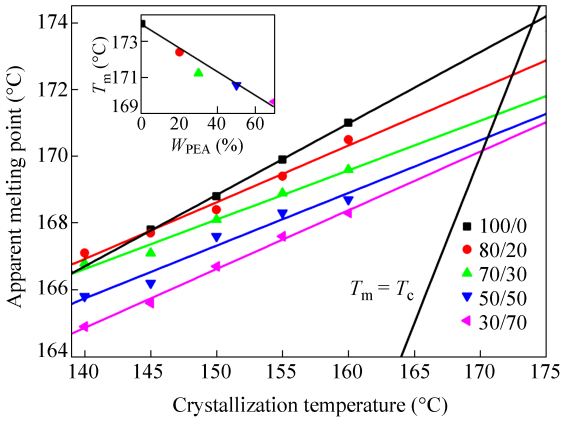


Fig. 2 Hoffman-Weeks plots for PVDF/PEA blends The inset-plot shows the composition dependence of equilibrium melting point T_m^0 obtained by Hoffman-Weeks plots.

caused by the thermodynamic effect. The equilibrium melting temperature can be derived by the following Hoffman-Weeks equation[27]

$$T_m = \eta T_c + (1-\mu)T_m^0 \tag{1}$$

where the slope of the Hoffman-Weeks plot, η, may be regarded as a measure of the stability of the crystals. According to the equation, the intersect of T_c versus T_m with the line defined by $T_c = T_m$ should yield T_m^0. Figure 2 shows the Hoffmann-Weeks plots for the pure PVDF with different blend compositions. The T_m^0 obtained by Hoffman-Weeks plots are shown as a function of PEA content in the inset-plot of Fig. 2. The T_m^0 of pure PVDF obtained here is 174 °C. However, T_m^0 of PVDF in PVDF/PEA blends decreases slightly with PEA content. The maximum depression of the melting point is 4.5 K in the 30/70 blend, where the T_m^0 of the PVDF is 169.5 °C. This indicates that PVDF is miscible with PEA to some extent.

Then, from the equilibrium melting temperature of each of the blend compositions, the intermolecular interaction parameter, χ_{12} can be estimated by Nishi-Wang equation, which was originally based on the Flory-Huggins theory[28]:

$$\frac{1}{T_m} - \frac{1}{T_m^0} = -\frac{RV_2}{\Delta H_f V_1}\left[\frac{\ln\varphi_2}{m_2} + \left(\frac{1}{m_2} - \frac{1}{m_1}\right)\varphi_1 + \chi_{12}\varphi_1^2\right] \tag{2}$$

where the subscript 1 stands for the component (PEA), which does not crystallize within the temperature range of interest and subscript 2 represents the crystalline polymer (PVDF). T_m and T_m^0 are the equilibrium melting points of the blends and neat PVDF. ΔH_f signifies the heat of fusion of PVDF per monomeric unit. V is the molar volume of the repeating unit, φ stands for volume fractions, m is the degree of polymerization, and R is the universal gas constant. By rearranging the terms of Eq. (2) we obtain:

$$-\left[\frac{\Delta H_f V_1}{RV_2}\left(\frac{1}{T_m} - \frac{1}{T_m^0}\right) + \frac{\ln\varphi_2}{m_2} + \left(\frac{1}{m_2} - \frac{1}{m_1}\right)\varphi_1\right] = \beta = \chi_{12}\varphi_1^2 \tag{3}$$

If the interaction parameter χ_{12} is independent of the blend composition, there will be a linear relationship between β and φ_1^2. Thus χ_{12} is obtained from the slope of the straight line. In order to calculate the Eq. (3), the following parameter values were used: ΔH_f = 5962 J/mol, V_1 = 145.4 cm^3/mol, V_2 = 36.4 cm^3/mol, m_1 = 58, m_2 = 4297. Weight fractions were converted to volume fractions using ρ(PVDF) = 1.78 g/cm^3 and ρ(PEA) = 1.18 g/cm^3.

The plot of Eq. (3) obtained by using the experimental value of T_m (blend) and T_m^0 (PVDF) is shown in Fig. 3. A negative but quite small value of χ_{12} is obtained (–0.02) for the PVDF/PEA blend, which indicates that although PVDF may show miscibility with PEA to some extent, the interaction strength is quite weak. A comparison with other blends shows that for the PVDF/PBA blend, $\chi_{PVDF\text{-}PBA}$ = –0.19[16]; for PVDF/PBS, $\chi_{PVDF\text{-}PBS}$ = –0.14[29]. Obviously, the interaction between PVDF and PEA is much weaker than that between PVDF and PBS (or PBA). So, the degree of miscibility of PVDF/PEA blends is lower than PVDF/PBS or PVDF/PBA blends. The carbonyl groups in the three polyesters that are capable of forming hydrogen bonds or exerting dipole-dipole interactions with the CH_2 or CF_2 groups of PVDF may be responsible for the miscibility of the three PVDF/carbonyl-containing polyester blend systems. However, the change in the structure of the polyester constituent results in the difference in the interaction strength[26].

Isothermal Crystallization Kinetics

The isothermal crystallization kinetics of PVDF/PEA blends was investigated by DSC. Two crystallization temperatures were selected: 150 °C for PVDF and 33 °C for PEA. Figure 4 shows the typical curves of relative crystallinity dependence of crystallization time for PVDF component at 150 °C (a) and PEA component at 33 °C

(b). It can be seen that the characteristic sigmoidal shape was obtained for all the samples. It was first Avrami[30] who showed that in isothermal conditions; the change in crystallinity with time can be monitored by thermal analysis (DSC) through the evolution of crystallization heat and readily expressed in the equation:

$$1-X_t = \exp(-kt^n) \tag{4}$$

where X_t is the relative crystallinity at crystallization time t, k is a rate constant depending on nucleation and crystalline growth rate, and n is the Avrami exponent which denotes the nature of the nucleation and growth process. Eq. (4) can be rewritten as:

$$\lg[-\ln(1-X_t)] = \lg k + n\lg t \tag{5}$$

A plot of $\lg[-\ln(1-X_t)]$ versus $\lg t$ gives a straight line from which both rate constant and the Avrami exponent can be derived. Figure 5 presents Avrami plots of PVDF/PEA blends at crystallization temperatures of 150 °C (a) and 33 °C (b) for PVDF and PEA components, respectively. A series of straight lines are obtained, which suggests that Avrami equation can adequately describe the isothermal crystallization kinetics of PVDF/PEA blends.

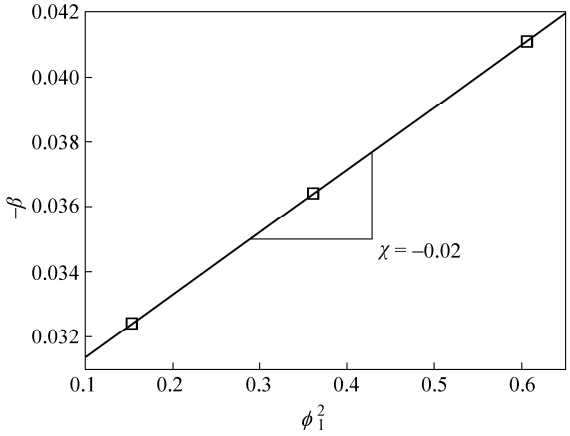


Fig. 3 Plot of β versus φ_1^2 according to the Flory-Huggins's equation

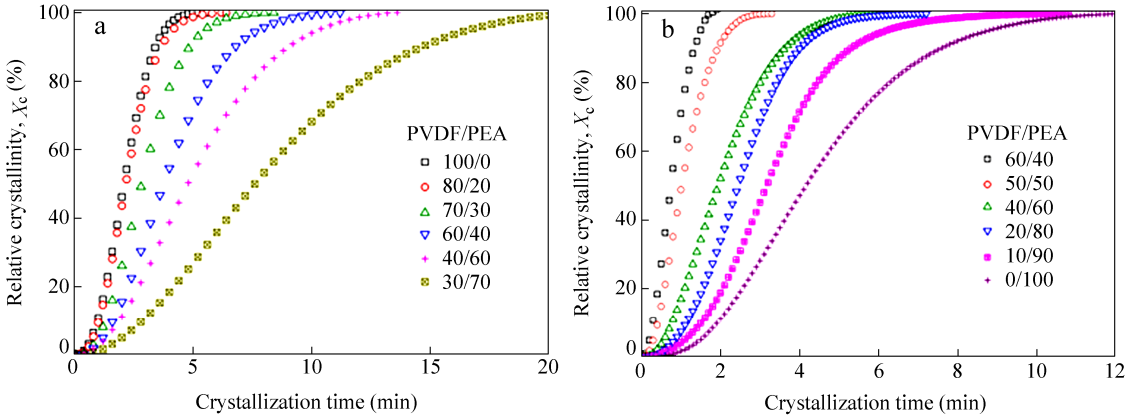


Fig. 4 Plots of relative crystallinity versus crystallization time for PVDF at 150 °C (a) and PEA at 33 °C (b) in PVDF/PEA blends during isothermal crystallization

From the straight lines of the Avrami plots, the Avrami exponent n and crystallization rate constant k were obtained, and the results are listed in Table 1. The Avrami exponent n is around 2.5 for neat PVDF while in the PVDF/PEA blends it is around 2, indicating that the presence of PEA affects the crystallization mechanism of PVDF. The Avrami exponent n is around 2.7 for neat PEA while in the PVDF/PEA blends it is around 2, suggesting that the presence of PVDF crystals also changes the crystallization mechanism of PEA in the blends.

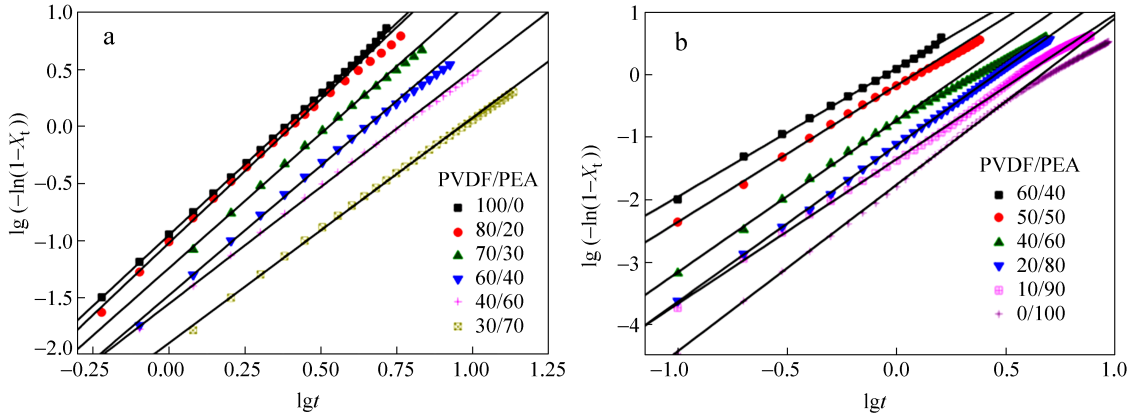


Fig. 5 Avrami plots of PVDF isothermally crystallized at 150 °C (a) and PEA isothermally crystallized at 33 °C (b)

The half-time of crystallization ($t_{0.5}$), defined as the time needed to achieve 50% of the final crystallinity, is an important parameter to describe isothermal crystallization kinetics. The value of $t_{0.5}$ can be obtained by:

$$t_{0.5} = \left(\frac{\ln 2}{k}\right)^{1/n} \tag{6}$$

Recoprocal value of $t_{0.5}$ (*i.e.*, $1/t_{0.5}$) is usually employed to describe the overall crystallization rates of polymers. According to the values of n and k listed in Table 1, the values of $t_{0.5}$ and $1/t_{0.5}$ were calculated and plotted in Fig. 6 as a function of blend composition. As shown in Fig. 6(a), the value of $t_{0.5}$ for PVDF increases with PEA. On the other hand, the value of $1/t_{0.5}$ decreases with the addition of PEA. The results are consistent with the trend of k listed in Table 1.

Table 1. Parameters n and k from the Avrami analysis of isothermal melt crystallization for PVDF and PEA in PVDF/PEA blends

	PVDF/PEA	n	k (min^{-n})
PVDF	100/0	2.47	1.12×10^{-1}
	80/20	2.52	9.57×10^{-2}
	70/30	2.36	5.77×10^{-2}
	60/40	2.27	3.34×10^{-2}
	40/60	2.05	2.81×10^{-2}
	30/70	1.97	1.27×10^{-2}
PEA	60/40	2.06	1.27
	50/50	2.19	6.74×10^{-1}
	40/60	2.44	1.87×10^{-1}
	20/80	2.5	7.41×10^{-2}
	10/90	2.32	4.47×10^{-2}
	0/100	2.67	1.74×10^{-2}

All the aforementioned results can lead us to a conclusion that the addition of PEA not only changes the overall crystallization mechanism of PVDF, but also reduces the crystallization rate in the PVDF/PEA blend. The reduction of crystallization rate of PVDF is mainly caused by the depression of the melting point after adding PEA content in blends. First, the equilibrium melting point of blended PVDF is about 4.5 K lower than that of neat PVDF, which may drop the thermodynamic driving force required for the growth of PVDF spherulites. Second, the added PEA may play a role of a diluent to PVDF in the miscible blends, resulting in the dilution of PVDF chains at the spherulites growth front.

Meanwhile, as seen in Fig. 6(b), the value of $1/t_{0.5}$ for PEA increases with the addition of PVDF in the blends, which is consistent with the trend of k for PEA listed in Table 1. In blends containing 60 wt% PVDF, the

overall crystallization is approximately 5.5 times faster than it is for neat PEA. In the case of PEA crystallization at 33 °C, PEA must crystallize within the matrix of pre-existing PVDF crystals formed at 150 °C. The crystallization rate of PEA in the PVDF/PEA blend increases with the addition of PVDF crystals, indicating that the pre-existing PVDF crystals act as the nucleating agents for PEA. The PVDF crystal provides a foreign surface where heterogeneous nucleation of PEA can take place, which lead to much higher nucleation rate for PEA.

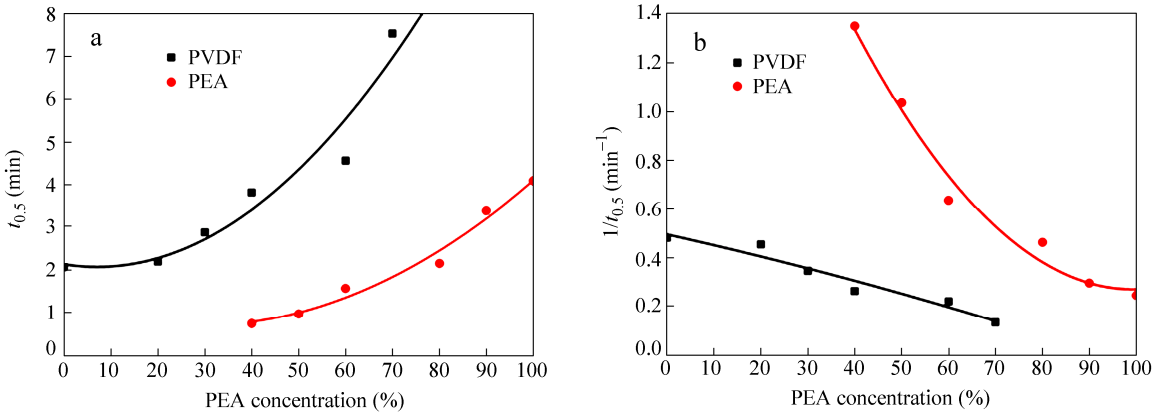


Fig. 6 $t_{0.5}$ (a) and $1/t_{0.5}$ (b) of PVDF and PEA in PVDF/PEA blends

Furthermore, the degree of crystallinity of PVDF decreases with increasing the PEA composition (see Fig. 7). The degree of crystallinity of neat PEA is around 53%. The low concentration of PVDF cannot affect the crystallinity of PEA. For PVDF/PEA 20/80 blend, the degree of crystallinity of PEA is around 51%. However, the crystallinity degree of PEA decreases sharply in the PVDF-rich blend. The results illustrate that at low concentration of PVDF in the blends PVDF increases the crystallization rate of PEA and not enhances the crystallinity of PEA. In the case of a high ratio of PVDF in the blends, although PVDF crystals act as nucleates to promote the crystallization of PEA, the confinement of crystals dominates the crystallization and results in the low crystallinity of PEA.

To check the crystalline structure of PVDF and PEA in the PVDF/PEA blend, wide-angle X-ray diffraction measurements were performed on the samples used for Fig. 4. Figure 8 shows the X-ray diffraction patterns of the PVDF/PEA blends. The patterns of the blends are just the superimposition of the pure PVDF and PEA patterns, indicating that the two components have not mutually influenced their crystalline structure.

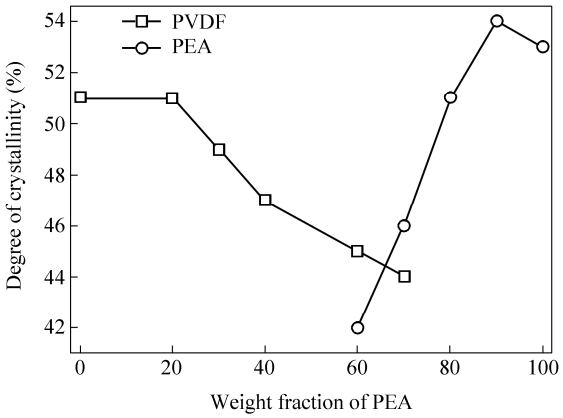


Fig. 7 Degree of crystallinity of PVDF and PEA in the PVDF/PEA blend with different blend ratios

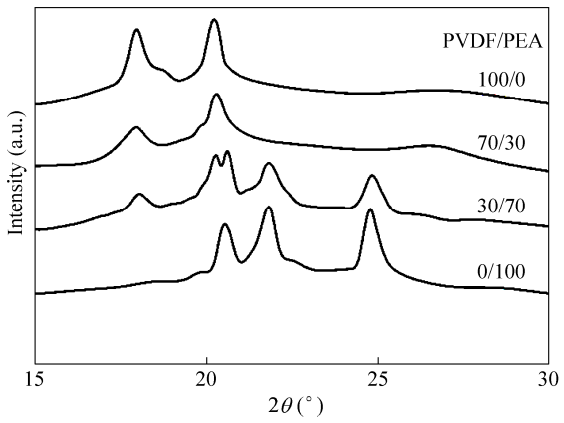


Fig. 8 WAXD patterns of pure PVDF, pure PEA, and their blends with different blend ratios (Before the measurement, PVDF was crystallized at 150 °C and PEA was crystallized at 33 °C.)

Non-isothermal Crystallization

PVDF has a T_m of 168 °C, while PEA has a T_m of 50 °C. Because of the large difference in T_ms of the two components, it is impossible for the two components to crystallize simultaneously. When a PVDF/PEA blend is slowly cooled from the melt, PVDF crystallizes first followed by crystallization of PEA. Figure 9 shows DSC cooling traces of PVDF/PEA blends at 10 K/min from the homogeneous melt (a) and subsequent melting behavior at 10 K/min (b). As seen in Fig. 9(a), the crystallization temperature of PVDF is found at 140 °C, which shifts to low-temperature ranges with increasing the PEA content and decreases to 136 °C for 10/90 blend. The decrease of crystallization temperature of PVDF is related to the depression of T_m^0 of PVDF and the diluting effect of PEA.

However, the crystallization behavior of PEA is a little complicated. As shown in Fig. 9(a), during the cooling process of neat PEA, a broad and weak crystallization peak emerges from 15 °C to –20 °C. In the subsequent heating process as shown in Fig. 9(b), neat PEA exhibits a strong exothermic cold crystallization peak at 0 °C before it is melted. This indicates that during the cooling process at 10 K/min, most of PEA does not crystallize and remains amorphous. However, during the cooling process, the PEA component in the PVDF/PEA blend crystallizes completely in a wide temperature range, from 20 °C to –10 °C. Furthermore, the main crystallization peak of PEA (T_c) shifts to high temperatures with increasing the PVDF content. T_c of PEA shifts to 8.2 °C for the 30/70 blend from 0 °C for the 10/90 blend. When the PVDF content is increased to 50%, T_c of PEA shifts to 17 °C and keeps unchanged with further increasing the PVDF content. The above results indicates that the pre-existing PVDF crystals act as the nucleating agents for PEA and increase its crystallization temperature during the cooling process, which is coincident with the isothermal crystallization kinetically results.

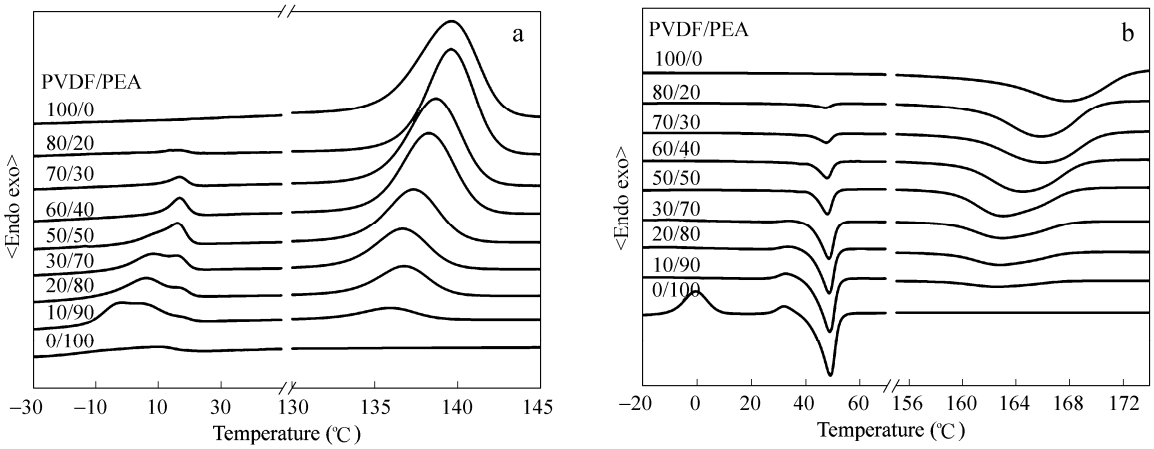


Fig. 9 DSC cooling traces of PVDF/PEA blends at 10 K/min from the homogeneous melt (a) and subsequent melting behavior at 10 K/min (b)

Figure 9(b) shows the subsequent melting behavior of the PVDF/PEA blends at 10 K/min after they finished the nonisothemal crystallization as shown in Fig. 9(a). The melting temperature (T_m) of neat PEA is at around 50 °C and shifts to low temperatures slightly with increasing the PVDF content. Similarly, it can be also found that T_m of PVDF decreases with the addition of PEA. T_m of PVDF shifts from 168 °C for neat PVDF to 163 °C for 10/90 blend. The melting point depressions of PEA in their blends further indicated their miscibility.

Crystalline Morphologies of PVDF/PEA Blends

As discussed above, the crystallization kinetics of each component is affected by the existence of the other component in PVDF/PEA blends. So it is expected that the crystalline morphology of one component would also be affected by the other. In the present study, the crystalline morphologies of PVDF/PEA blends are studied by POM and SEM *via* a two-stage crystallization procedure, *i.e.*, crystallization of PVDF at 150 °C and

subsequent crystallization of PEA at 33 °C.

Figure 10(a) shows the POM image of the spherulitic morphology of neat PVDF crystallized at 150 °C. As seen in Fig. 10(a), the spherulites of PVDF show the familiar maltese cross birefringent pattern and exhibit concentric extinction bands. These spherulites characterized by high birefringence and concentric banding comprise α-form crystals[6]. Figure 10(b) shows the POM micrograph of neat PEA melt-crystallized at 33 °C. It can be clearly observed that PEA formed ring-banded spherulites. Figures 10(c), 10(e) and 10(g) show the POM images of the spherulitic morphologies of PVDF in various blends after complete crystallization at 150 °C. As PEA is added to PVDF, the α-form spherulites become progressively larger since fewer nuclei are formed. As seen in Fig. 10(e), when the PEA content is increased to 50%, the diluting effect of PEA on PVDF becomes evident and many non-birefringent domains form within PVDF spheruliltes. When PEA content reaches 70%, the PVDF spherulites remain relatively space filling (Fig. 10g). This indicates that a substantial portion of molten PEA melt is first rejected into the interlamellar or interfibrillar regions during the crystallization process of PVDF.

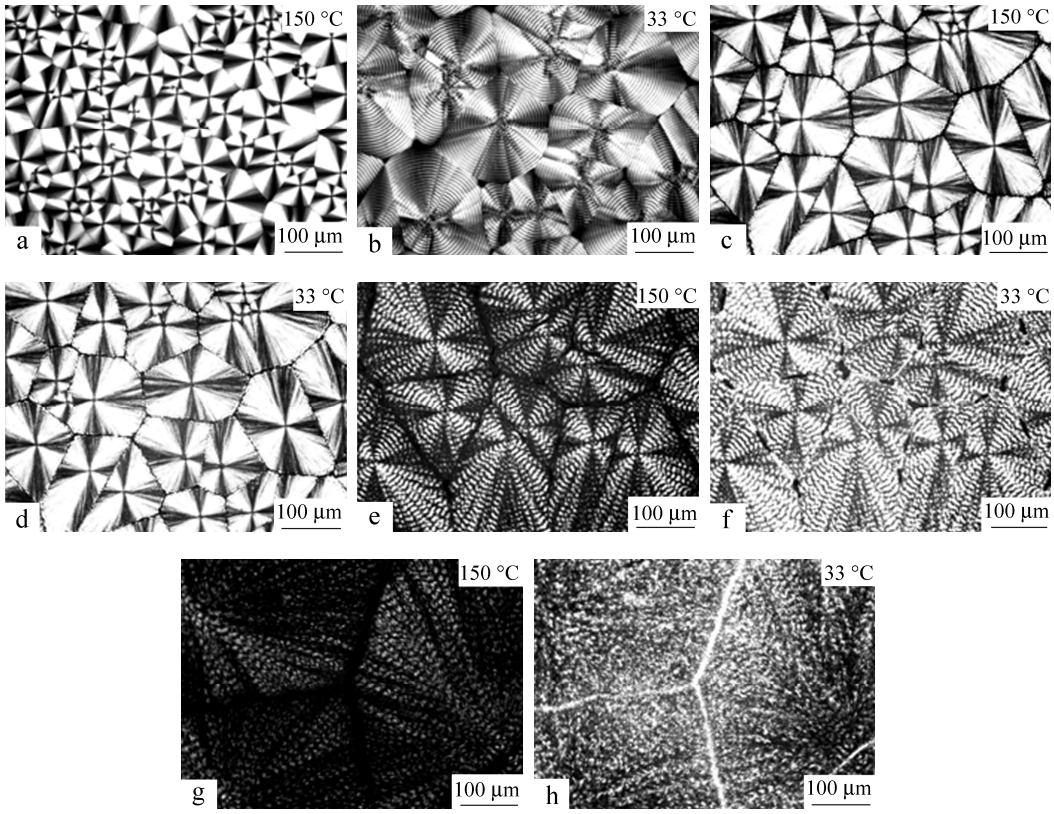


Fig. 10 Optical micrographs of the spherulitic morphologies of PVDF/PEA blends: (a) neat PVDF, (b) neat PEA, (c, d) 70/30, (e, f) 50/50 and (g, h) 30/70 PVDF/PEA blends

In addition, the band spacing of the PVDF spherulite increases with PEA content (Figs. 10c and 10e). Similarly, the band spacing of PVDF in PVDF/PBA and PVDF/PHBV blends also increases with increasing the noncrystallizing component[16, 21]. Banding spherulitic structures with regular concentric rings along radial direction are commonly observed in polymeric spherulites and are believed to arise from cooperative twisting of radiating lamellar crystals around their axis of fastest growth. For a certain polymer system, the band spacing usually increases with decreased supercooling[10, 11]. As a diluent, PEA results in a lower supercooling of PVDF in the blends, since the equilibrium melting point is decreased. As a result, the bandwidth of the α-form PVDF

spherulite becomes larger with the addition of PEA. Meanwhile, it is noted that the band spacing in the margin areas of the α-form spherulites is significantly larger than that in core region, which shows that an amount of PEA is expelled to the spherulitic growth front at the advanced stages of crystallization. After complete crystallization, the nonbirefringence appears in the interspherulitic regions, indicating that part of PEA is finally expelled into the interspherulitic region.

During cooling, no birefringent changes have been identified at temperatures above the melting point of PEA, indicating the completion of crystallization of PVDF at 150 °C for 72 h. Therefore, the morphological change during further cooling process is mainly caused by the crystallization of the PEA component. When the blends are cooled from the semicrystalline/amorphous state to a temperature below the melting point of PEA, the crystallization of this component will bring the PVDF/PEA blend system into the semicrystalline/semicrystalline state. Figures 10(d), 10(f) and 10(h) illustrate the morphological changes after cooling the blend from 150 °C to 33 °C. The birefringence of the sample changes markedly, reflecting the crystallization of PEA. In addition, the intensity of the birefringence increases in both intraspherulitic and interspherulitic regions. This helps us to conclude that the PEA component is dispersed in the intraspherulitic and interspherulitic regions. However, the *in situ* observation of crystallizaton process indicates that crystallization of PEA initially takes place in the interspherulitic region of PVDF and then proceeds in the intraspherulitic region. For the PEA component, the crystal growth based on a spherulitic morphology is not observed. This nonspherical growth habit of PEA in PVDF matrix should be attributed to two factors. On the one hand, lots of pre-existing PVDF crystals act as the nucleating agents for PEA, which increases greatly the nucleation density of PEA. On the other hand, once the nucleation is finished, the further growth of PEA lamellae is greatly hindered by PVDF crystals.

Although the POM results clearly reveal the influence of PEA on the spherulitic morphology of PVDF, we cannot get the fine structural information due to the resolution limit. Therefore, for a better understanding of the morphological details of the PVDF/PEA blend systems, a further study of the internal structures of PVDF spherulites is necessary. Figure 11 shows the SEM micrographs of spherulitic morphologies of neat PVDF melt-crystallized at 150 °C. Figure 11(a) reveals that the α-form PVDF spherulite is composed of the twisting lamellar bundles that are viewed alternately edge-on and face-on. The bright bands consist of edge-on lamellar bundles while the dark ones consist of lamellar bundles seen face-on. The lamellar twisting is discontinuous and quite abrupt. The periodic distance of rings was measured to be about 2.2 μm. This is more clearly seen in the magnified image (Fig. 11b).

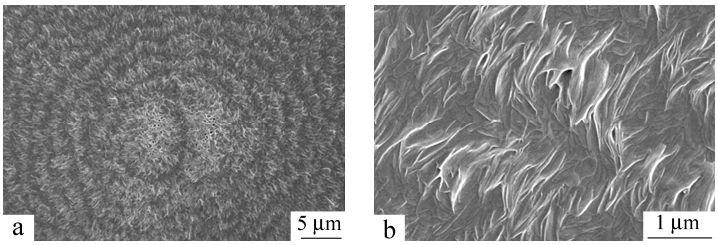


Fig. 11 SEM images of PVDF isothermally crystallized at 150 °C for 72 h

Figure 12 shows the spherulitic morphologies of PVDF/PEA blends crystallized at 150 °C. In order to observe lamellar structure of PVDF more clearly, the PEA component has been etched away by chloroform. Figures 12(a) and 12(b) show the SEM graphs of the top free surface morphologies of 70/30 and 30/70 PVDF/PEA blends, respectively. As was often observed in other spherulite species, a spiral structure is seen at the core of the banded spherulite. Many disturbances in concentric bands are noticed through careful observation of the ring-banded structure. With the increment of PEA, these disturbances become more obvious. The spiral and discontinuous structure is caused by rhythmic crystal growth theoretically explained by the time-dependent Ginzburg-Landau equation in which the coupling of compositional ordering and orientational crystal ordering

are considered[31, 32]. Additionally, the inter-ring spacing of the PVDF component increases to 5 μm with an addition of 30% PEA. But with an addition of 70% PEA, the spacing increases to 10 μm. This result is in agreement with the POM observations, as shown in Figs. 8(b) and 8(d). Additionally, deep holes are frequently found in the regions between edge-on lamellar stacks on the top surface of the banded spherulite (Figs. 12c and 12d). The holes become progressively larger with increasing PEA concentration, indicating that these holes are attributed to an amorphous pocket of PEA extracted by the etching with chloroform. Figures 12(e) and 21(f) show SEM graphs for the fractured surface of 70/30 and 30/70 PVDF/PEA blends. As seen in the two Figures, the α-form spherulites are mainly composed of the bundles of radial lamellae. These lamellar bundles are mutually parallel, and exhibit characteristics of layered structure, indicating that lamellar bundles twist collaboratively. Furthermore, it can be noted that the lamellar bundles are well separated and the distance between lamellar bundles increases with PEA concentration, suggesting that the PEA component is expelled into the pockets between the lamellar bundles during the crystallization process of the PVDF component. So the subsequent crystallization of PEA is restricted in these isolated pockets. The interlamellar or interfibrillar phase segregation of PEA makes its molecular chains so difficult to diffuse from one isolated micro-domain to another that PEA cannot crystallize into spherulitic structure.

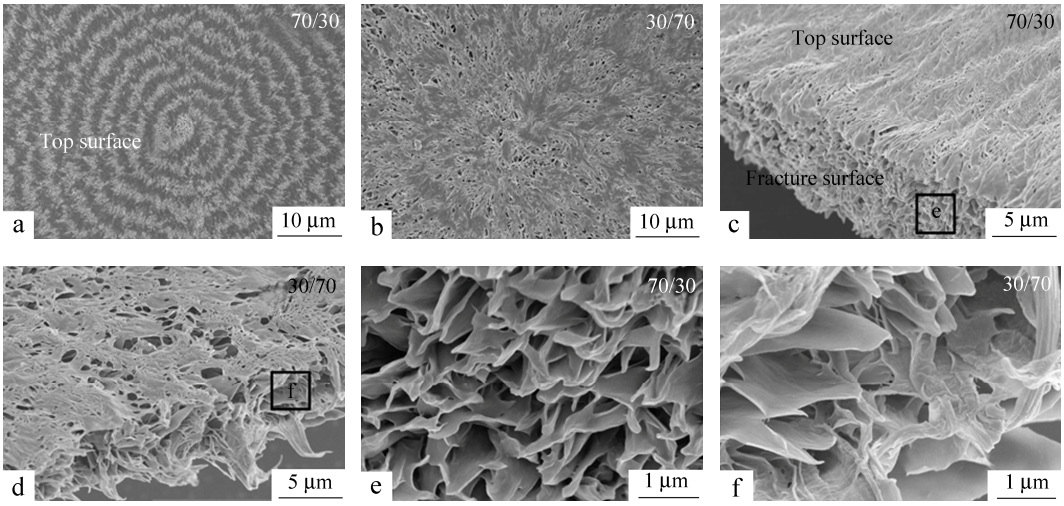


Fig. 12 SEM graphs of spherulitic morphologies of PVDF in the 70/30 (a, c and e) and 30/70 (b, d and f) PVDF/PEA blends crystallized at 150 °C

Another phenomenon for particular attention is that the lateral dimension of lamellar bundles is also affected by the blend ratio. The comparison of Figs. 12(e) and 12(f) reveals that, in the 70/30 blend, the width of the lamellar bundles in the lateral direction was less than one micron, but in the 30/70 blend, the width increased to several micrometers. In essence, the lamellar twisting of PVDF originates from unbalanced surface stresses[33]. As evidenced in Fig. 12, the inter-ring spacing increases with content of the PEA component, indicating that the unbalanced surface stress in favor of lamellar twisting is probably reduced in the PVDF/PEA blend.

In addition to the blend ratio, the crystallization temperature also affects the spherulitic morphology of PVDF in the PVDF/PEA blend. Figure 13 shows POM and SEM images of spherulitic morphology of PVDF in a 30/70 PVDF/PEA blend melt-crystallized at 130 °C. The scaffolds of PVDF are highly branched and quite open, exhibiting an irregular and interconnected network. As a result, the PEA segregations (etched portions) are not restricted in isolated regions and form interconnected phases. In this case, the crystallization of PEA is different from that in the 30/70 blend melt-crystallized at 150 °C. Figure 14 shows the crystallization of PEA at 33 °C in the 30/70 blend shown in Fig. 13. As seen in Fig. 14, PEA is nucleated randomly and grows in ring-

banded spherulites. However, the band structure of PEA is unclear and irregular, which implies that the PEA lamellar synchronous twisting is often interrupted by the pre-existing PVDF crystals. Furthermore, the nucleation frequency of PEA crystallization is much lower than that of PVDF, requiring that the PEA spherulites grow through many tiny PVDF spherulites. In other words, the interpenetrated structure is formed by the penetration of PEA spherulites growing into PVDF spherulites.

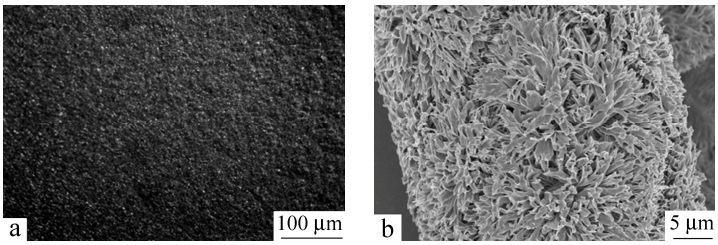


Fig. 13 POM (a) and SEM (b) graphs of spherulitic morphologies of PVDF in the 30/70 PVDF/PEA blends crystallized at 130 °C

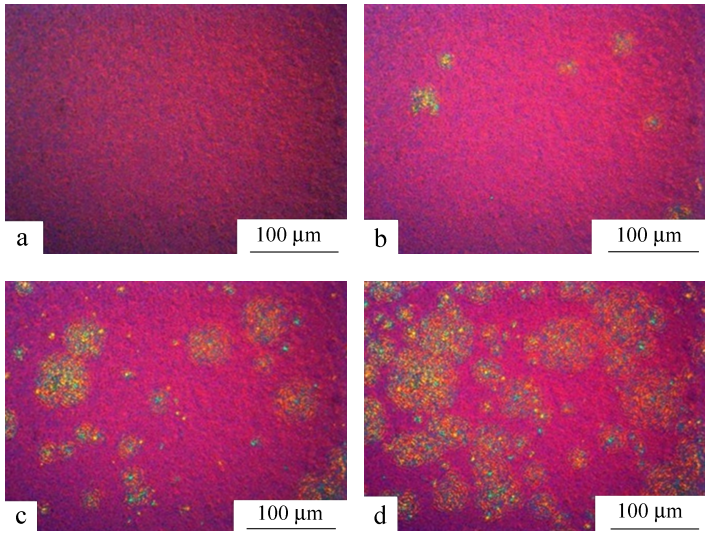


Fig. 14 POM images of a 30/70 PVDF/PEA blend crystallized at 130 °C and subsequently quenched to 33 °C for (a) 0 min, (b) 8 min, (c) 14 min and (d) 18 min

CONCLUSIONS

The miscibility, isothermal crystallization kinetics and morphologies of the poly(vinylidene fluoride) (PVDF)/poly(ethylene adipate) (PEA) blends have been studied systematically by DSC, OM and SEM. The equilibrium melting point of PVDF in the blends was obtained from DSC results using the Hoffman-Weeks equation and found to decrease with increasing PEA content. A negative but quite small interaction parameter is elucidated from melting point depression data, indicating that although PVDF is misible with PEA to some extent, the interaction strength is quite weak. The crystallization kinetics is greatly affected by the blend composition. The crystallization rate of PVDF decreases with the increment of PEA, which is mainly caused by the depression of the equilibrium melting point after adding PEA. However, the crystallization rate of PEA increases with PVDF contents, indicating that the pre-existing PVDF crystals act as nucleation agents for PEA. The blend ratio and crystallization temperature affect the texture of PVDF spherulites greatly, which determines the subsequent crystallization of PEA. At high temperatures, *e.g.* 150 °C, the band spacing of PVDF spherulites increases with the addition of PEA content and the spherulitic structure becomes more open. The PEA

component is expelled into the isolated pockets between the lamellar bundles of PVDF. In this case, spherulitic crystallization of PEA is not observed for all blend compositions. At low temperatures, *e.g.* 130 °C, for PEA-rich blends, the amorphous regions between the PVDF lamellar bundles are well connected with each other. As a result, the interpenetrated structure is eventually formed by the penetration of the spherulites of PEA growing within the pre-existing PVDF spherulites.

REFERENCES

1 Penning, J.P. and Manley, R., St. J., Macromolecules, 1996, 29: 77
2 Pang, D.Z., Zuo, M., Zhao, J.S. and Zheng, Q., Chinese J. Polym. Sci., 2013, 31(11): 1470
3 Wang, L., Jiang, Z.W., Liu, F., Zhang, Z.J. and Tang, T., Chinese J. Polym. Sci., 2014, 32(3): 333
4 Zou, F.S., Dong, X., Liu, W., Wang, D.J. and Charles C.H., Chinese J. Polym. Sci., 2014, 32(6): 718
5 Wu, D.D., Li, W., Liang, H.Y., Liu, S.R., Fang, J.Y., Zhang, H.L., Zhang, H.X. and Dong, L.S., Chinese J. Polym. Sci., 2014, 32(7): 914
6 Lovinger, A.J., J. Polym .Sci. Polym. Phys. Ed., 1982, 18: 793
7 Morra, B.S. and Stein, R.S., J. Polym. Sci. Polym. Phys. Ed., 1988, 21: 2243
8 Léonard, C., Halary, J.L. and Monnerie, L., Macromolecules, 1988, 21: 2988
9 Saito, H. and Stühn, B., Macromolecules, 1994, 27: 216
10 Okabe, Y., Murakami, H., Osaka, N., Saito, H. and Inoue, T., Polymer, 2010, 51: 1494
11 Okabe, Y., Kyu, T., Saito, H. and Inoue, T., Macromolecules, 1998, 31: 5823
12 Okabe, Y. and Kyu, T., Polymer, 2004, 45: 8485
13 Rahman, M.H. and Nandi, A.K., J. Polym. Sci., Part B: Polym. Phys., 2004, 42: 2215
14 Na, B., Xu, W.F., Lv, R.H., Li, Z.J., Tian, N.N. and Zou, S.F., Macromolecules, 2010, 43: 3911
15 Isayeva, I., Kyu, T. and Manley, R.St.J., Polymer, 1998, 39: 4599
16 Penning, J.P. and Manley, R.St.J., Macromolecules, 1996, 29: 77
17 Liu, L.Z., Chu, B., Penning, J.P. and Manley, R.St.J., Macromolecules, 1997, 30: 4398
18 Yang, J.J., Pan, P.J., Hua, L., Zhu, B., Dong, T. and Inoue, Y., Macromolecules, 2010, 43: 8610
19 Lee, J.C., Ikehara, T., Nishi, T. and Tazawa, H., Polymer J., 1998, 30: 327
20 Qiu, Z.B., Fujinami, S., Komura, M., Nakajima, K., Ikehara, T. and Nishi, T., Polymer, 2004, 45: 4355
21 Qiu, Z.B., Yan, C.Z., Lu, J.M., Yang, W.T., Ikehara, T. and Nishi, T., J. Phys. Chem. B, 2007, 111: 2783
22 Wang, T.C., Li, H.H., Wang, F., Yan, S.K. and Schultz, J.M., J. Phys. Chem. B, 2011, 115: 7814
23 Wang, T.C., Li, H.H. and Yan, S.K., Chinese J. Polym. Sci., 2012, 30(2): 269
24 Svoboda, P., Trivedi, K., Svobodova, D., Mokrejs, P., Vasek, V., Mori, K., Ougizawa, T. and Inoue, T., Macromol. Chem. Phys., 2011, 131: 84
25 Yan, C.Z., Guo, L., Chang, H.B. and Yan, S.K., Chinese J. Polym. Sci., 2013, 31(8): 1173
26 Li, S.H. and Woo, E.M., J. Appl. Polym. Sci., 2008, 107: 766
27 Hoffman, J.D. and Weeks, J.J., J. Res. Nat. Bur. Stand. A. Phys. Chem., 1962, 66A: 13
28 Nishi, T. and Wang, T.T., Macromolecules, 1975, 8: 909
29 Lee, J.C., Tazawa, H., Ikehara, T. and Nishi, T., Polymer J., 1998, 30: 327
30 Avrami, M., J. Chem. Phys., 1939, 7: 1103
31 Okabe, Y., Kyu, T., Saito, H. and Inoue, T., Macromolecules, 1998, 31: 5823
32 Kyu, T., Chiu, H.W., Guenthner, A.L., Okabe, Y., Saito, H. and Inoue, T., Phys. Rev. Lett., 1999, 83: 2749
33 Lotz, B. and Cheng, S.Z.D., Polymer, 2005, 46: 577